



**Queensland University of Technology**  
Brisbane Australia

This is the author's version of a work that was submitted/accepted for publication in the following source:

Yang, Liuliu, Shi, Guodong, Ke, Xuebin, Shen, Ruwei, & Zhang, Lixiong (2014) Mesoporous titania microspheres composed of exposed active faceted nanosheets and their catalytic activities for solvent-free synthesis of azoxybenzenes. *CrystEngComm*, 16(9), pp. 1620-1624.

This file was downloaded from: <http://eprints.qut.edu.au/67145/>

© Copyright 2014 The Royal Society of Chemistry

**Notice:** *Changes introduced as a result of publishing processes such as copy-editing and formatting may not be reflected in this document. For a definitive version of this work, please refer to the published source:*

<http://dx.doi.org/10.1039/C3CE42252F>

Cite this: DOI: 10.1039/c0xx00000x

www.rsc.org/xxxxxx

ARTICLE TYPE

# Mesoporous titania microspheres composed of exposed active faceted nanosheets and their catalytic activities for solvent-free synthesis of azoxybenzenes

Liuliu Yang,<sup>a</sup> Guodong Shi,<sup>a</sup> Xuebin Ke,<sup>b</sup> Ruwei Shen<sup>a</sup> and Lixiong Zhang<sup>\*a</sup>

<sup>5</sup> Received (in XXX, XXX) Xth XXXXXXXXX 20XX, Accepted Xth XXXXXXXXX 20XX  
DOI: 10.1039/b000000x

Mesoporous titania microspheres composed of nanosheets with exposed active facets were prepared by hydrothermal synthesis in the presence of hexafluorosilicic acid. They exhibited superior catalytic activity in the solvent-free synthesis of azoxybenzene by oxidation of aniline and could be used for 7 cycles with slight loss of activity.

Titanium dioxide (TiO<sub>2</sub>) has been intensively investigated in the last couple of decades since its relative low cost and widely application in many areas such as photocatalysis, energy conversion and storage, sensor, catalyst, and catalyst support.<sup>1</sup> It is generally synthesized as nanoparticles and nano/microspheres. TiO<sub>2</sub> with other morphologies, such as disks,<sup>2</sup> rods,<sup>3</sup> wires<sup>4</sup> and tubes,<sup>5</sup> is also produced, as these morphologies can endow unique properties of TiO<sub>2</sub>. Recently, TiO<sub>2</sub> with highly exposed crystal facets and with these exposed facet crystal-constructed hierarchical structures has attracted much attention. Various techniques are developed to prepare these kinds of TiO<sub>2</sub>, mainly by hydrothermal or solvothermal treatment of titanium precursor solutions synthesis in the presence of fluorine ion<sup>6,7</sup> and capping reagents such as ammonia,<sup>8</sup> H<sub>2</sub>O<sub>2</sub>,<sup>9</sup> alcohols,<sup>10</sup> etc, or by hydrothermal treatment of titania powder, nanowires or nanotubes in acid/basic solutions.<sup>11</sup> Further results demonstrate that expose of {001}, {110}, {010}, {111}, {102}, {106} and {103} facets can enhance the reactivity of TiO<sub>2</sub>, especially in photocatalysis and dye-sensitive solar cells (DSSCs).<sup>12</sup> Similarly, TiO<sub>2</sub> with the exposed facet crystal-constructed V-shaped channels,<sup>13</sup> nanosheets or nanorods assembly,<sup>14,15</sup> core-shell,<sup>16</sup> sphere-in-sphere,<sup>17</sup> and dandelion-like<sup>18</sup> hierarchical structures exhibit outstanding performance in DSSCs, lithium ion batteries, and photocatalysis.

As a versatile catalytic material, TiO<sub>2</sub> is mostly used as photocatalysts and a support of both metal and oxide catalysts in heterogeneous catalysis. A few work use nano-sized TiO<sub>2</sub> as heterogeneous catalysts mainly for organic synthesis, such as Michael addition of indoles to  $\alpha,\beta$ -unsaturated ketones,<sup>19</sup> Mannich synthesis of  $\beta$ -aminocarbonyls,<sup>20</sup> synthesis of substitute 2-oxodihydropyrroles and bis(indolyl)methanes,<sup>21</sup> etc. It is interesting that there are limited work on use TiO<sub>2</sub> as a catalyst for catalytic oxidation reactions, although titanium containing materials, such as titanium-substituted molecular

sieves,<sup>22</sup> are good catalysts for this kind of reaction. Oxidations of amines with H<sub>2</sub>O<sub>2</sub> to oximes and azoxybenzenes are the main two reactions reported so far using the nano-sized TiO<sub>2</sub> as the catalysts in which solvents such as acetone, CH<sub>3</sub>CN, CH<sub>3</sub>OH, etc, are used to achieve good yields.<sup>23,24</sup> It would be of both academic and industrial interest to examine the catalytic oxidation activity of these TiO<sub>2</sub> with highly exposed crystal facets or with hierarchical structures.

Aromatic azo compounds are high-value intermediates for production of dyes, pigments, food additives, and drugs.<sup>25</sup> Reduction of nitroaromatics and oxidation of anilines are the main route to prepare these compounds. Oxidation of anilines can be carried out with oxygen at high pressures or H<sub>2</sub>O<sub>2</sub> under mild conditions. From a practical viewpoint, a mild reaction is more favorable. As mentioned above, nano-sized TiO<sub>2</sub> exhibits excellent catalytic activity in oxidation anilines to azoxybenzenes, however, a solvent has to be used. Synthesis of azoxybenzene by oxidation of aniline with H<sub>2</sub>O<sub>2</sub> without a solvent provides a green and mild route and needs to be developed.

Herein, we reported preparation of mesoporous TiO<sub>2</sub> microspheres (MTMs) with particle size of 2-15  $\mu$ m composed of TiO<sub>2</sub> nanosheets (side length of 10-20 nm, thickness of 4-6 nm) with exposed {101} facet (56%) by a simple hydrothermal synthesis. The microspheres exhibited superior catalytic activities in solvent-free oxidation of arylamines to azoxybenzenes rather than azobenzene. To the best of our knowledge, no such application of exposed facet crystal-constructed hierarchical TiO<sub>2</sub> structures in heterogeneous catalysis has been reported.

The MTMs were hydrothermally synthesized at 180 °C for 48 h using a synthesis solution with a molar ratio of 1TBOT: 0.1H<sub>2</sub>SiF<sub>6</sub>: 1.5H<sub>2</sub>O prepared by adding a H<sub>2</sub>SiF<sub>6</sub> aqueous solution into TBOT under vigorous stirring (ESI†). Fig.1a shows XRD patterns of the as-synthesized sample, indicating formation of pure anatase TiO<sub>2</sub> (tetragonal, *I41/amd*, JCPDS No. 21-1272). The diffraction peaks at  $2\theta$  of 25.3°, 37.8°, and 48.5° can be observed obviously, corresponding to (101), (004) and (200) faces of TiO<sub>2</sub>. The peak intensity at  $2\theta=25.3^\circ$  is much stronger than those at 37.8° and 48.5°, implying the preferred growth along (101) face.<sup>26</sup> The primary crystallite size calculated from the (101) peak of XRD pattern using the

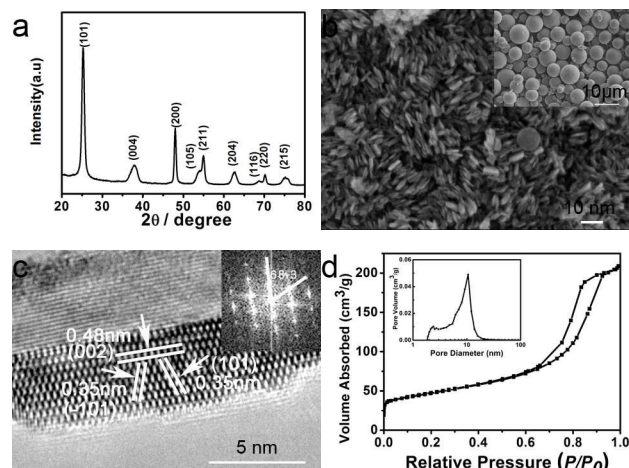


Fig. 1 XRD pattern (a), SEM images (b), TEM image (c) of the TiO<sub>2</sub> microspheres composed of nanosheets, recorded from anatase single nanocrystal with the corresponding fast-Fourier transform (FFT) pattern in the inset, and nitrogen adsorption-desorption isotherm and Barret-Joyner-Halenda (BJH) pore size distribution plot of the MTM (d).

scherrer equation is about 14.7 nm. XRD patterns of the samples synthesized at 2-96 h (Fig. S1, ESI†) indicate that the intensity of the (101) face becomes stronger with increasing the synthesis time and reaches the strongest at 48 h, indicating the highest crystallinity of the sample after synthesis for 48 h. Fig. 1b show SEM picture of the MTM. It exhibits spherical morphology with particle size of 2-12 μm (Inset in Fig. 1b). Close observations reveals that the microsphere is composed of compactly packed nanocrystals.

To elucidate the fine structure of nano-sized sheets, we examined the sample by TEM after grounding and ultrasound dispersing the sample. A representative high-resolution TEM image of a single nanosheet (Fig. 1c)<sup>27</sup> reveals that these nanosheets are well-faceted nanocrystals with side length of 10-20 nm and thickness of *ca.* 4.6 nm. The (-101), (101) and (002) atomic planes with lattice spacings of 0.35, 0.35 and 0.48 nm indicate that the top/bottom surface exposed by truncation is bound by a {001} facet.<sup>28,29</sup> The inset of Fig. 1c shows that the angle labeled in the corresponding fast-Fourier transform (FFT) image is 68.3±0.3°, which is identical to the theoretical value for the angle between the {101} and {001} facets.<sup>28</sup> These facets prove that the anatase single crystals exhibit flat facets of {101} and {001}. On the basis of the above structural information, the percentage of {001} facets in the TiO<sub>2</sub> nanosheets shown in Fig. 1c is estimated to be 44% according to eq. 1.<sup>30</sup> Correspondingly, the percentage of {101} is 56%.

$$\frac{a^2}{(b^2 - a^2) + a^2} \times 100\% \quad (1)$$

Where, *a* is the side length of {001} facet, *b* the bottom edge of {101} facet and *θ* the value for the angle between the {101} and {001} facets.

The nitrogen adsorption-desorption isotherm was measured to determine the specific area and pore volume of the MTM. The corresponding results were presented in Fig. 1d. The pore size distribution, derived from desorption data

and calculated using the BJH model, indicated that the average pore of such a sample is around 10.2 nm. The Brunauer–Emmett–Teller (BET) specific surface area of the sample calculated from N<sub>2</sub> adsorption is 117 m<sup>2</sup> g<sup>-1</sup>, which is larger than those of conventionally prepared TiO<sub>2</sub> microsphere.<sup>13,15</sup> The much higher BET surface area of the MSM may provide the possibility of contacting active center more effectively.

To investigate the elemental compositions and the binding states of the MTM, the sample was analyzed by XPS (Fig. S3, ESI†). Sharp photoelectron peaks appear at binding energies of 458 (Ti 2p) and 531 eV (O 1s). The F 1s peak at 684.5 eV is observed due to surface fluorination. High-resolution XPS was used to detect the surface F 1s, Ti 2p, and O 1s core levels. No signals for F<sup>-</sup> in the lattice (BE = 688.5 eV) is found after the MTM was calcined at 600 °C, implying that all F<sup>-</sup> is physically adsorbed on the surface of the MTM, and does not substitute of oxygen in TiO<sub>2</sub> lattice. The binding energy of Ti 2p<sub>3/2</sub> equals to 458.7 eV and the binding energy of Ti 2p<sub>1/2</sub> equals to 464.4 eV, which are identical to the reported literature.<sup>31</sup> These results confirm that titanium exists as Ti (IV) state. The O 1s peak at 530.2 eV indicates oxygen in Ti–O–Ti. No Si peak (101.8 eV) is observed, suggesting that Si in H<sub>2</sub>SiF<sub>6</sub> does not enter into or adsorb on the MTM.

Table 1 Oxidation of arylamines to azoxybenzenes in the presence of TiO<sub>2</sub>/H<sub>2</sub>O<sub>2</sub> system.

Entry	Arylamine	Time (h)	Conversion (%)	Yield (%)
1	<chem>Nc1ccccc1</chem>	0.75	97.8	95.6
2	<chem>Nc1ccccc1C</chem>	2	98.7	94.5
3	<chem>Nc1ccc(C)cc1</chem>	4.5	91.0	86.5
4	<chem>Nc1ccc(OC)cc1</chem>	4.5	85.4	81.3
5	<chem>Nc1ccc(Cl)cc1</chem>	6.0	80.8	75

(catalyst = 25 mg; arylamines = 0.02 mol; arylamines/H<sub>2</sub>O<sub>2</sub> molar ratio = 1:1.7; temperature = 333 K)

The MTM shows quite high catalytic activity in the catalytic oxidation of arylamines with H<sub>2</sub>O<sub>2</sub> to azoxybenzenes. In particular, no solvent is used in these reaction systems, unlike the reported system for conversion of aniline H<sub>2</sub>O<sub>2</sub> to azoxybenzene, in which acetone, CH<sub>3</sub>CN, CH<sub>3</sub>OH, are usually used as solvent,<sup>23,24</sup> implying a green catalytic synthesis route. Table 1 listed the reaction results of oxidation of some arylamines with H<sub>2</sub>O<sub>2</sub>. It is observed from that aniline results in a good yield of azoxybenzene within a shorter reaction when compared with the substituted anilines, while toluidines are more reactive than the chloro or methoxy substituted anilines. This may be attributed to the smaller size of toluidine atoms, which would allow the reactant molecules to gain closer proximity to the active centers on the titanium peroxo species compared to the larger chlorine atoms or methoxy groups. However, the differences in the reactivity of various substituted anilines are dependent on the synergetic

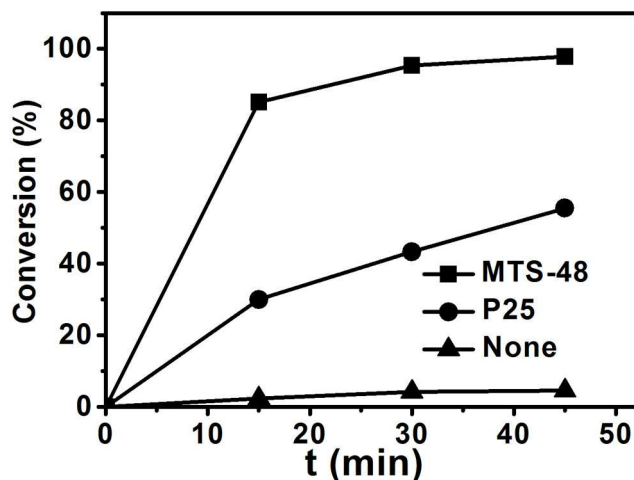


Fig. 2 Effect of reaction time on aniline conversion and azoxybenzene yield with MTM and P25 and without a catalyst. (catalyst =25mg; aniline=1.86 g; aniline/H<sub>2</sub>O<sub>2</sub> molar ratio=1:1.7; temperature=333 K)

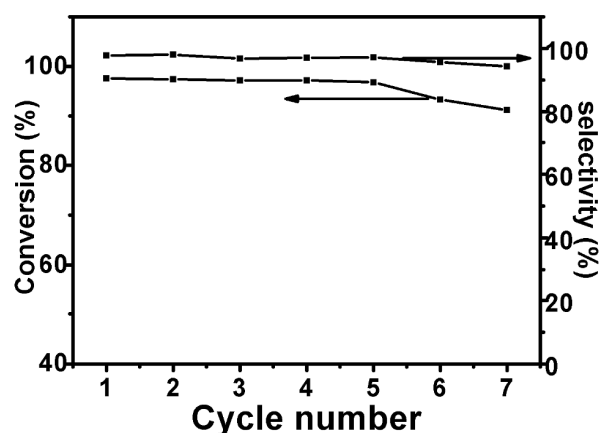


Fig. 3 Cycling curve for aniline oxidation with the MTM as the catalyst.

effect of the molecular parameters such as mesomeric (+M), inductive (+I/-I) and the steric effect of the substituents.<sup>24</sup> Furthermore, it should be noted that no obvious difference was observed on the conversion of aniline and the yield of azoxybenzene when the reaction was conducted with or without sun light irradiation, clearly suggesting that MTM does not act as a photocatalyst in the present reaction.

To compare the catalytic property of the TiO<sub>2</sub> microspheres with TiO<sub>2</sub> powder P25 (Degussa), we conducted time-dependent kinetics of aniline with H<sub>2</sub>O<sub>2</sub> using the MTM and P25 as the catalysts. Blank test without a catalyst was also conducted. The reaction results shown in Fig. 2 clearly demonstrate that this reaction goes on a quite slow reaction rate with low conversion of aniline without a catalyst. Increasing the reaction time directly increases the aniline conversion using the MTM and P25. The reaction rate of the MTM is significantly greater than that of P25. The yield of azoxybenzene increases smoothly with the reaction time for 30 min to 45 min. After 45 min, the aniline conversion reaches a maximum value of 97.8% and the yield of azoxybenzene is up to 95.6%, which are much higher than those by P25.

Fig. 3 shows that after 6 recycling uses, the activity of the MTM remains above 93.3% with selectivity of azoxybenzene being 95.6%, which indicates that the exposed crystal-facets TiO<sub>2</sub> microspheres have high catalytic stability in the oxidation of arylamine. A slight loss of the catalytic activity was observed in the 7th recycling use (conversion: 91.2%, selectivity: 94.3%).

To identify the contributions of the {101} facets and hierarchical structure of the MTM on the aniline oxidation, diverse samples with varying percentages of exposed {101} facets were prepared by changing the synthesis time, and the results of aniline oxidation to azoxybenzene on these samples were listed in Table 2 (Entries 1 and 2). By extending the synthesis time to 72 and 96 h at 180 °C, the percentages of {101} facets of the MTM are 47% to 37%, respectively. This is similar to the result reported by Yang, et al.<sup>6a</sup>. The conversion of aniline and the yield of azoxybenzene are slightly decreased, suggesting possibly more active sites on the MTM with higher percentage of {101} facet. To examine the effect of hierarchical structure of the MTM on the aniline oxidation, we ground the MTM sample to form mostly nanosheets. Even with an increase in the percentage of {101} facet (56%), the conversion still decreases slightly (entry 3), possibly due to lack of hierarchical structure. To further elucidate the effect, the anatase TiO<sub>2</sub> nanosheet-based microspheres (ATNM)<sup>15</sup> and anatase TiO<sub>2</sub> nanoparticle-based hierarchical spheres (ATNHS)<sup>29</sup>, as well as titania nanosheets (NS)<sup>7</sup> were also prepared, with the {101} facet percentage of 94%, 10%, and 20%, respectively. The results indicated that the samples with hierarchical structures and both very high or low {101} facet percentage (entries 4 and 5) exhibit quite low conversions and yields, while the sample with very low {101} facet percentage shows slightly low conversion and yield (entry 6), compared with those for the MTM. These results suggested that both the {101} facet percentage and the hierarchical structure of the MTM play significant roles in oxidation of aniline. To obtain much higher catalytic activity, TiO<sub>2</sub> catalysts with mediate {101} facet percentages as well as the hierarchical structure have to be used (entries 1 and 2 in Table 2).

Table 2 Oxidation of aniline to azoxybenzene at different catalyst

Entry	Catalyst	Conversion (%)	Yield (%)	P(101) %	hierarchical structure
1	MTM <sup>a</sup>	94.5	90.9	47	yes
2	MTM <sup>b</sup>	93.6	89.6	37	yes
3	MTM <sup>c</sup>	91.4	89.3	56	no
4	ATNM	22.6	21.0	94	yes
5	ATNHS	61.8	58.4	10	yes
6	NS	87.3	85.4	20	no

<sup>a</sup> The MTM sample synthesized at 180 °C for 72 h; <sup>b</sup> The MTM sample synthesized at 180 °C for 96 h; <sup>c</sup> The MTM sample synthesized at 180 °C for 48 h and ground into mostly nanosheets. The reaction time is 0.75 h.

In conclusion, we developed a new approach to synthesize anatase mesoporous TiO<sub>2</sub> microsphere composed of nanosheets with exposed {101} facet (56%) by a simple hydrothermal synthesis using H<sub>2</sub>SiF<sub>6</sub>. The microsphere shows high conversion and yield in oxidation of arylamines to azoxybenzenes with H<sub>2</sub>O<sub>2</sub> without a solvent at mild conditions. Both the appropriate proportion of {101} and



{001} facets and the hierarchical structure of the MTM contribute the high reaction activity. The MTM provides an environment-friendly and easily recyclable heterogeneous catalytic route for the preparation of azoxybenzene.

## 5 Notes and references

<sup>a</sup> State Key Laboratory of materials-oriented Chemical Engineering, College of Chemistry and Chemical Engineering, Nanjing University of Technology, Nanjing, China. Fax: +86 25 83172263; Tel: +86 25 83172265; E-mail: lixiongzhong@yahoo.com

<sup>b</sup> School of Chemistry, Physics and Mechanism Engineering, Queensland University of Technology, Brisbane, Qld 4001, Australia.

† Electronic Supplementary Information (ESI) available: Experimental Detail, XRD pattern, XPS spectra. See DOI: 10.1039/b000000x/

- 1 (a) X. B. Chen, S. S. Mao, *Chem. Rev.*, 2007, **107**, 2891; (b) U. Diebold, *Surf. Sci. Rep.*, 2003, **48**, 53; (c) D. V. Bavykin, J. M. Friedrich and F. C. Walsh, *Adv. Mater.*, 2006, **18**, 2807; (d) Z. Y. Zhou, N. Tian, J. T. Li, I. Broadwell and S. G. Sun, *Chem. Soc. Rev.*, 2011, **40**, 4167.
- 2 A. Y. Zhang, M. H. Zhou, L. Han and Q. X. Zhou, *J. Hazard. Mater.*, 2011, **186**, 1374.
- 3 Y. W. Jun, M. F. Casula, J. H. Sim, S. Y. Kim, J. Cheon and A. P. Alivisatos, *J. Am. Chem. Soc.*, 2003, **125**, 15981.
- 4 Y. B. Mao, S. S. Wong, *J. Am. Chem. Soc.*, 2006, **128**, 8217.
- 5 T. Kasuga, M. Hiramatsu, A. Hoson, T. Sekino and K. Niihara, *Langmuir*, 1998, **14**, 3160.
- 6 (a) H. G. Yang, C. H. Sun, S. Z. Qiao, J. Zou, G. Liu, S. C. Smith, H. M. Cheng and G. Q. Lu, *Nature*, 2008, **453**, 638; (b) D. Q. Zhang, G. S. Li, X. F. Yang and J. C. Yu, *Chem. Commun.*, 2009, **29**, 4381; (c) J. Pan, G. Liu, G. Q. Lu and H. M. Cheng, *Angew. Chem. Int. Ed.*, 2011, **50**, 2133;
- 7 X. G. Han, Q. Kuang, J. M. Shang, Z. X. Xie and L. S. Zheng, *J. Am. Chem. Soc.*, 2009, **131**, 3152.
- 8 (a) C. T. Dinh, T. D. Nguyen, F. Kleitz and T. O. Do, *ACS Nano*, 2009, **3**, 3737; (b) X. Y. Ma, Z. G. Chen, S. B. Hartono, H. B. Jiang, J. Zou, S. Z. Qiao and H. G. Yang, *Chem. Commun.*, 2010, **46**, 6608; (c) B. H. Wu, C. Y. Guo, N. Zheng, Z. X. Xie and G. D. Stucky, *J. Am. Chem. Soc.*, 2008, **130**, 17563; (d) X. K. Ding, H. C. Ruan, C. Zheng, J. Yang and M. D. Wei, *CrystEngComm*, 2013, **15**, 3040; (e) H. Xu, P. Reunchan, S. X. Ouyang, H. Tong, N. Umezawa, T. Kako and J. H. Ye, *Chem. Mater.*, 2013, **25**, 405.
- 9 (a) X. L. Wang, H. L. He, Y. Chen, J. Q. Zhao and X. Y. Zhang, *Appl. Surf. Sci.*, 2012, **258**, 5863; (b) M. Liu, L. Y. Piao, L. Zhao, S. T. Ju, Z. J. Yan, T. He, C. L. Zhou and W. J. Wang, *Chem. Commun.*, 2010, **46**, 1664; (c) Y. G. Miao, J. C. Gao, *J. Solid State Chem.*, 2012, **196**, 372;
- 10 (a) H. G. Yang, G. Liu, S. Z. Qiao, C. H. Sun, Y. G. Jin, S. C. Smith, J. Zou, H. M. Cheng and G. Q. Lu, *J. Am. Chem. Soc.*, 2009, **131**, 4078; (b) J. M. Du, J. S. Zhang and D. J. Kang, *CrystEngComm*, 2011, **13**, 4270; (c) J. Zhu, S. H. Wang, Z. F. Bian, S. H. Xie, C. L. Cai, J. G. Wang, H. G. Yang and H. X. Li, *CrystEngComm*, 2010, **12**, 2219; (d) W. G. Yang, Y. L. Wang and W. M. Shi, *CrystEngComm*, 2012, **14**, 230.
- 11 (a) W. Li, Y. Bai, W. J. Liu, C. Liu, Z. H. Yang, X. Feng, X. H. Lu and K. Y. Chan, *J. Mater. Chem.*, 2011, **21**, 6718; (b) J. M. Li, D. S. Xu, *Chem. Commun.*, 2010, **46**, 2301; (c) M. Miyauchi, *J. Mater. Chem.*, 2008, **18**, 1858.
- 12 P. H. Wen, Y. Ishikawa, H. Itoh and Q. Feng, *J. Phys. Chem. C*, 2009, **113**, 20275.
- 13 H. Pan, J. S. Qian, Y. M. Cui, H. X. Xie and X. F. Zhou, *J. Mater. Chem.*, 2012, **22**, 6002.
- 14 (a) J. S. Chen, Y. L. Tan, C. M. Li, Y. L. Cheah, D. Luan, S. Madhavi, F. Y. C. Boey, L. A. Archer and X. W. Lou, *J. Am. Chem. Soc.*, 2010, **132**, 6124; (b) G. Liu, J. Pan, L. C. Yin, J. T. Irvine, F. Li, J. Tan, P. Wormald and H. M. Cheng, *Adv. Funct. Mater.*, 2012, **22**, 3233; (c) J. Zhu, J. G. Wang, F. J. Lv, S. X. Xiao, C. Nuckolls and H. X. Li, *J. Am. Chem. Soc.*, 2013, **135**, 4719; (d) J. M. Li, K. Cao, Q. Li and D. S. Xu, *CrystEngComm*, 2012, **14**, 83.
- 15 W. G. Yang, J. M. Li, Y. L. Wang, F. Zhu, W. M. Shi, F. R. Wan and D. S. Xu, *Chem. Commun.*, 2011, **47**, 1809.
- 16 (a) B. S. Liu, K. Nakata, M. Sakai, H. Saito, T. Ochiai, T. Murakami, K. Takagi and A. Fujishima, *Catal. Sci. Technol.*, 2012, **2**, 1933; (b) B. S. Liu, K. Nakata, M. Sakai, H. Saito, T. Ochiai, T. Murakami, K. Takagi and A. Fujishima, *Langmuir*, 2011, **27**, 8500.
- 17 H. X. Li, Z. F. Bian, J. Zhu, D. Q. Zhang, G. S. Li, Y. N. Huo, H. Li and Y. F. Lu, *J. Am. Chem. Soc.*, 2007, **129**, 8406.
- 18 H. B. Wu, J. S. Chen, X. W. Lou and H. H. Hng, *Nanoscale*, 2011, **3**, 4082.
- 19 A. Fischer, P. Makowski, J. O. Muller, M. Antonietti, A. Thomas and F. Goettmann, *ChemSusChem*, 2008, **1**, 444.
- 20 M. Z. Kassae, R. Mohammadi, H. Masrouri and F. Movahedi, *Chin. Chem. Lett.*, 2011, **22**, 1203.
- 21 M. L. Kantam, S. Laha, J. Yadav, B. M. Choudary and B. Sreedhar, *Adv. Synth. Catal.*, 2006, **348**, 867.
- 22 (a) A. Tuel, S. Gontier and R. Teissier, *Chem. Commun.*, 1996, 651; (b) Y. S. S. Wan, K. L. Yeung and A. Gavruilidis, *Appl. Catal. A*, 2005, **281**, 285; (c) S. Gontier, A. Tuel, *J. Catal.*, 1995, **157**, 124; (d) S. Gontier, A. Tuel, *Appl. Catal. A*, 1996, **143**, 125; (e) H. R. Sonawane, A. V. Pol, P. P. Moghe, S. S. Biswas and A. Sudalai, *J. Chem. Soc., Chem. Commun.*, 1994, 1215.
- 23 (a) W. K. Chan, C. M. Ho, M. K. Wong and C. M. Che, *J. Am. Chem. Soc.*, 2006, **128**, 14796; (b) C. F. Chang, S. T. Liu, *J. Mol. Catalysis A: Chem.*, 2009, **299**, 121; (c) N. Jagtap, V. Ramaswamy, *Appl. Clay Sci.*, 2006, **33**, 89.
- 24 H. Tumma, N. Nagaraju and K. V. Reddy, *Appl. Catal. A*, 2009, **353**, 54.
- 25 (a) S. Sakuae, T. Tsubakino, Y. Nishiyama and Y. Ishii, *J. Org. Chem.*, 1993, **58**, 3633; (b) A. B. E. Vix, P. M. Buschbaum, W. Stocker, M. Stamm and J. P. Rabe, *Langmuir*, 2000, **16**, 10456.
- 26 R. L. Penn and J. F. Banfield, *Geochem. Cosmochim. Acta*, 1999, **63**, 1549.
- 27 For the low-resolution TEM images of MTM synthesized at 48 h, see Fig. S2.
- 28 Y. Q. Dai, C. M. Cobley, J. Zeng, Y. M. Sun and Y. N. Xia, *Nano Lett.*, 2009, **9**, 2455.
- 29 D. H. Wang, J. Liu, Q. S. Huo, Z. M. Nie, W. G. Lu, R. E. Williford and Y. B. Jiang, *J. Am. Chem. Soc.*, 2006, **128**, 13670.
- 30 Y. B. Zhao, W. H. Ma, Y. Li, H. W. Ji, C. C. Chen, H. Y. Zhu and J. C. Zhao, *Angew. Chem.*, 2012, **124**, 3242.
- 31 (a) J. C. Yu, J. G. Yu, W. K. Ho, Z. T. Jiang and L. Z. Zhang, *Chem. Mater.*, 2002, **14**, 3808; (b) D. Li, H. Haneda, S. Hishita and N. Ohashi, *Chem. Mater.*, 2005, **17**, 2596.